

A Fictitious Time Integration Method for Multi-Dimensional Backward Heat Conduction Problems

Chih-Wen Chang¹

Abstract: In this article, we propose a new numerical approach for solving these multi-dimensional nonlinear and nonhomogeneous backward heat conduction problems (BHCPs). A fictitious time τ is employed to transform the dependent variable $u(x, y, z, t)$ into a new one by $(1+\tau)u(x, y, z, t) =: v(x, y, z, t, \tau)$, such that the original nonlinear and nonhomogeneous heat conduction equation is written as a new parabolic type partial differential equation in the space of (x, y, z, t, τ) . In addition, a fictitious viscous damping coefficient can be used to strengthen the stability of numerical integration of the discretized equations by utilizing a group preserving scheme. Six numerical experiments illustrate that the present algorithm can be employed to recover the initial data very well. Even under the very large noisy final data, the fictitious time integration method is also robust against noise.

Keywords: Backward heat conduction problem, Strongly ill-posed problem, Heat conduction equation, Fictitious time integration method (FTIM), Group preserving scheme

1 Introduction

In many pragmatic application fields such as archeology, it requires to find the temperature history from the known final data. This is the so-called backward heat conduction problem (BHCP), which is a strongly ill-posed problem because the solution is unstable for the given final data. The aim of this research is to study these multi-dimensional nonlinear and nonhomogeneous BHCPs. Many methods have been proposed for solving the homogeneous BHCPs. Han, Ingham and Yuan (1995) utilized the boundary element method with a minimal energy technique to resolve the homogeneous BHCP; however, a large amount of computer storage is needed when the final time T is large or when the dimensions are higher. After that, the iterative boundary element method for the homogeneous BHCP was used by

¹ Grid Applied Technology Division, National Center for High-Performance Computing, Taichung 40763, Taiwan. Tel.: +886-4-24620202x860. E-mail address: 0903040@nchc.narl.org.tw

Lesnic, Elliott and Ingham (1998), Mera, Elliott, Ingham and Lesnic (2001), Mera, Elliott and Ingham (2002), and Jourhmane and Mera (2002). They reported that the scheme was efficient in recovering the temperature history even if a large value was employed for the final time, at which the temperature was fixed. Apart from this, Muniz, de Campos Velho and Ramos (1999) proposed an explicit inversion method and a sequential scheme of inversion to cope with the homogeneous BHCP. However, these two approaches did not give good results even with a small final time $T = 0.008$. Later, Muniz, Ramos and de Campos Velho (2000) adopted the Tikhonov regularization, maximum entropy principle and truncated singular value decomposition to resolve the homogeneous BHCP with good results, but their recovery time $T = 0.01$ is also small. Besides, the operator-splitting methods have been developed to tackle the BHCP [Kirkup and Wadsworth (2002)], similar to the Jacobi and related approaches for the iterative solution of a linear system of equations, and they claimed that their schemes were simple and remarkably effective. Nevertheless, the retrieved time $T = \log 2 / \pi^2$ is still too small. Liu (2002) proposed the regularized successive over-relaxation (SOR) inversion and the direct SOR inversion. He claimed that the regularized SOR is stable even under the influence of a high noise level, but its recovery time is only 5×10^{-3} . On the contrary, the direct SOR inversion is unstable for small noises. Subsequent to Liu (2002), Iijima (2004) established a high order lattice-free finite difference method by using the Fourier transform and Taylor expansion. Nevertheless, this study did not discuss how the final time data were disturbed by noise. After that, Mera (2005) employed the method of fundamental solutions (MFS) and the standard Tikhonov regularization technique to tackle the BHCP. In that article, he mentioned that the MFS is an accurate and reliable technique for solving the homogeneous BHCP in one-dimensional and higher dimensional domains; however, the standard Tikhonov regularization technique with the L-curve method is still required for a numerical stability reason. Recently, Tsai, Young and Kolibal (2010) have used the time evolution method of MFS to resolve the homogeneous BHCP without any regularization techniques.

Recently, Liu, Chang and Chang (2006) and Liu (2006a) have utilized the backward group preserving scheme (BGPS) to tackle the homogeneous BHCP and backward in time Burgers equation, respectively. Lack of need for a priori regularization in use, makes the BGPS more appealing for inverse problems with a final value problem. Actually the BGPS was an extension of the work by Liu (2004) by taking time regression of equations into account in the formation of backward group theory. In the paper of Liu (2004), the group preserving scheme (GPS) was first adopted to deal with the homogeneous BHCP because the GPS [Liu (2001)] was an effective numerical approximation for solving nonlinear differential equations. The homogeneous BHCP has been solved by using the BGPS [Liu, Chang and Chang (2006)],

and the Lie-group shooting method (LGSM) [Chang, Liu and Chang (2007)] to a moderate time span, and the fictitious time integration method (FTIM) [Chang and Liu (2010a)] to a long time span, and Liu (2004) employed two transformations to resolve these homogeneous BHCPs; nevertheless, he did not consider how the final time data were affected by noises. Later, Liu, Chang and Chang (2006) proposed an explicit single-step algorithm to resolve these homogeneous BHCPs, but they could not tackle these homogeneous BHCPs with time varying boundary conditions very well when there were noisy final data. Recently, Chang, Liu and Chang (2007) and Chang, Liu and Chang (2009) have used the numerical implementation of quasi-reversibility together with the time-direction LGSM to solve the homogeneous BHCP and obtained good results. Besides, Chang, Liu and Chang (2010a) and Chang, Liu and Chang (2010b) utilized the quasi-boundary semi-analytical approach to tackle these homogeneous BHCPs and achieved nearly exact solutions. A recent review of the numerical BHCP was provided by Chiwiacowsky and de Campos Velho (2003).

For those multi-dimensional nonlinear and nonhomogeneous BHCPs, Long and Dinh (1994) proposed the regularization method to tackle the nonlinear BHCP, but its maximum error is quite large over 0.2. After that, Feng, Qian and Fu (2008) used the Tikhonov regularization method to deal with the nonhomogeneous BHCP. However, this approach did not give good results even with a small final time $T = 0.1$. Later, the quasi-reversibility method for the nonhomogeneous BHCP was employed by Trong and Tuan (2006). Although the approach gave good results, the retrieved time $T = 0.5$ is still small. Nevertheless, Trong and Tuan (2009a) used a method of integral equation to resolve the nonlinear BHCP, and they reported that regularized results are better than their previous results [Trong, Quan, Khanh and Tuan (2007); Trong and Tuan (2008b)]. Apart from this, Trong and Tuan (2008a) proposed a simple and convenient regularization method to tackle the nonhomogeneous BHCP. However, they reported that the regularized results are better than their previous results [Trong and Tuan (2006)]. For the two-dimensional (2-D) BHCP, Trong and Tuan (2009b) employed a truncated Fourier series method to solve the 2-D nonlinear BHCP, but this approach was complicated. After that, Tuan and Trong (2009) adopted a new regularized method to deal with the 2-D nonhomogeneous BHCP. In addition, Nam (2010) used the truncation method to tackle the nonlinear BHCP. Recently, Li, Jiang and Hon (2010) have proposed a meshless method based on RBFs method to solve 2-D and three-dimensional nonhomogeneous BHCPs, but this algorithm was complex and hard to implement. Without using a priori regularization, Chang and Liu (2010b) utilized the BGPS to tackle those multi-dimensional nonlinear and nonhomogeneous BHCPs and obtained good results.

This present article is summarized as follows. We describe the multi-dimensional nonlinear and nonhomogeneous BHCPs in the next section. In Section 3, we introduce a fictitious time coordinate τ by transforming the dependent variable $u(x, y, z, t)$ into a new one by $(1 + \tau)u(x, y, z, t) := v(x, y, z, t, \tau)$, such that the original equation is mathematically equivalently written as another different parabolic equation, where adding a fictitious viscous damping coefficient to enhance the stability of numerical integration of the discretized equations, and giving a concise sketch of GPS for ordinary differential equations (ODEs). Section 4 shows six instances to demonstrate the accuracy of the proposed approach. The most pivot conclusions from the current research are organized in Section 5.

2 Nonlinear and nonhomogeneous back heat conduction problems

The multi-dimensional nonlinear and nonhomogeneous BHCP we consider is respectively given by the following equations:

$$\frac{\partial u}{\partial t} = \Delta u + F(u) + g \text{ in } \Omega, \quad (1)$$

$$u = u_B \text{ on } \Gamma_B, \quad (2)$$

$$u = u_F \text{ on } \Gamma_F, \quad (3)$$

where u is a scalar temperature field of heat distribution, $F(u)$ is a nonlinear function of u , and g is the heat source. We take a bounded domain D in \mathbb{R}^j , $j = 1, 2, 3$ and a spacetime domain $\Omega = D \times (0, T)$ in \mathbb{R}^{j+1} for a final time $T > 0$, and write two surfaces $\Gamma_B = \partial D \times [0, T]$ and $\Gamma_F = \partial D \times \{T\}$ of the boundary $\partial\Omega$. Δ represents the j -dimensional Laplacian operator. While Eqs. (1)-(3) constitute a j -dimensional backward heat conduction problem for a given Dirichlet boundary data $u_B: \Gamma_B \mapsto R$ and a final time data $u_F: \Gamma_F \mapsto R$.

3 A fictitious time integration approach

3.1 Transformation into a different evolutionary PDE and semi-discretization

First, we propose the following transformation:

$$v(x, y, z, t, \tau) = (1 + \tau)u(x, y, z, t), \quad (4)$$

and introduce a fictitious viscosity damping coefficient $\psi > 0$ in Eq. (1):

$$0 = -\psi \frac{\partial u}{\partial t} + \psi \Delta u + \psi F(u) + \psi g. \quad (5)$$

Multiplying the above equation by $1 + \tau$ and employing Eq. (4), we have

$$0 = -\psi \frac{\partial v}{\partial t} + \psi \Delta v + \psi(1 + \tau)F(u) + \psi(1 + \tau)g. \tag{6}$$

Recalling that $\partial v / \partial \tau = u(x, y, z, t)$ by Eq. (4), and adding it on both the sides of the above equation we acquire

$$\frac{\partial v}{\partial \tau} = -\psi \frac{\partial v}{\partial t} + \psi \Delta v + \psi(1 + \tau)F(u) + \psi(1 + \tau)g + u. \tag{7}$$

Finally by employing $u = v/(1 + \tau)$, we can change Eqs. (1)-(3) into another parabolic type PDE:

$$\frac{\partial v}{\partial \tau} = -\psi \frac{\partial v}{\partial t} + \psi \Delta v + \psi(1 + \tau)F\left(\frac{v}{1 + \tau}\right) + \psi(1 + \tau)g + \frac{v}{1 + \tau} \text{ in } \tilde{\Omega}, \tag{8}$$

$$v = v_B \text{ on } \tilde{\Gamma}_B, \tag{9}$$

$$v = v_F \text{ on } \tilde{\Gamma}_F, \tag{10}$$

where $\tilde{\Omega} = \Omega \otimes [0, \tau_f]$, $\tilde{\Gamma}_B = \Gamma_B \otimes [0, \tau_f]$, $\tilde{\Gamma}_F = \Gamma_F \otimes [0, \tau_f]$ and τ_f is a selected value. In Eq. (8), τ is a fictitious time, being different to the real time t . Even though we raise these dimensions of Eq. (8) one higher than Eq. (1), several advantages can be gained as to be shown below.

There is maybe another selection of Eq. (4) by employing $v = p(\tau)u$, where we require that $p(\tau)$ be a monotonically increasing function of τ , $p(0) = 1$ and $p(\infty) = \infty$. However, when $p(\tau)$ is more complicated than $1 + \tau$ the resulting partial differential equation (PDE) is more complex than Eq. (8), and presently there seems no good reason to select a more complicated $p(\tau)$. However, other selections are possible if they can supply better result than the present one.

Applying a semi-discrete procedure to Eq. (8), yields a coupled system of ODEs:

$$\begin{aligned} \dot{v}_{i,j,k,\ell} = & \frac{-\psi}{\Delta t} [v_{i,j,k,\ell+1} - v_{i,j,k,\ell}] + \frac{\psi}{(\Delta x)^2} [v_{i+1,j,k,\ell} - 2v_{i,j,k,\ell} + v_{i-1,j,k,\ell}] \\ & + \frac{\psi}{(\Delta y)^2} [v_{i,j+1,k,\ell} - 2v_{i,j,k,\ell} + v_{i,j-1,k,\ell}] + \frac{\psi}{(\Delta z)^2} [v_{i,j,k+1,\ell} - 2v_{i,j,k,\ell} + v_{i,j,k-1,\ell}], \\ & + \psi(1 + \tau)F\left(\frac{v_{i,j,k,\ell}}{1 + \tau}\right) + \psi(1 + \tau)g_{i,j,k,\ell} + \frac{v_{i,j,k,\ell}}{1 + \tau}, \end{aligned} \tag{11}$$

where Δx , Δy and Δz are uniform spatial lengths in x , y and z directions, Δt is a time stepsize, $v_{i,j,k,\ell}(\tau) = v(x_i, y_j, z_k, t_\ell, \tau)$, and \dot{v} denotes the differential of v with respect to τ .

When one uses a suitable numerical integrator to integrate Eq. (11), a sequence of $v_{i,j,k,\ell}$ can be obtained. Given a stopping criterion, as shown below, to terminate the fictitious time stepping solution, we can acquire the solution of v at a fictitious time τ_f , and calculating u by Eq. (4), we can attain the solution of u in a fully spacetime region. Therefore, we call this novel approach a fictitious time integration method (FTIM).

The above concept by introducing a fictitious time was first proposed by Liu (2008a) to address an inverse Sturm-Liouville problem by transforming an ODE into a PDE. After that, Liu (2008b, 2008c) and Liu, Chang, Chang and Chen (2008) extended this idea to develop new methods for estimating parameters in the inverse vibration problems. More recently, Liu and his coworkers have employed the FTIM to solve many problems; see, e.g., Liu and Atluri (2008a) [nonlinear algebraic equations], Liu and Atluri (2008b) [discretized inverse sturm-Liouville problems], Liu (2008d) [nonlinear complementarity problems], Liu (2008e) [quasi-linear elliptic boundary value problems], Liu and Atluri (2008c) [mixed complementarity problems], Liu (2009a) [m -point boundary value problems], Liu (2009b) [delay ordinary differential equations], Liu (2009c) [a quasilinear elliptic boundary value problem with an arbitrary plane domain], Liu and Atluri (2009) [numerical solution of the Fredholm integral equation and numerical differentiation of noisy data, and its relation to the filter theory], Ku, Yeih, Liu and Chi (2009) [highly nonlinear boundary value problems], Chi, Yeih and Liu (2009) [Cauchy problem of Laplace equation], Chang and Liu (2009) [backward advection-dispersion equation], and Chang and Liu (2010a) [backward heat conduction problems].

3.2 GPS for differential equations system

We can write Eq. (11) as a vector form:

$$\dot{\mathbf{v}} = \mathbf{f}(\mathbf{v}, \tau), \quad \mathbf{v} \in \mathbb{R}^n, \quad \tau \in R, \quad (12)$$

where \mathbf{v} is an n -dimensional state vector, and $\mathbf{f} \in \mathbb{R}^n$ is a vector-valued function of \mathbf{v} and τ .

The GPS can preserve the internal symmetry group of the considered ODE system. For nonlinear differential equations systems, Liu (2001) has embedded them into the augmented dynamical systems, which concern with not only the evolution of state variables but also the evolution of the magnitude of state variables vector.

We can embed Eq. (12) into the following $n+1$ -dimensional augmented dynamical system:

$$\frac{d}{d\tau} \begin{bmatrix} \mathbf{v} \\ \|\mathbf{v}\| \end{bmatrix} = \begin{bmatrix} \mathbf{0}_{n \times n} & \frac{\mathbf{f}(\mathbf{v}, \tau)}{\|\mathbf{v}\|} \\ \frac{f^T(\mathbf{v}, \tau)}{\|\mathbf{v}\|} & 0 \end{bmatrix} \begin{bmatrix} \mathbf{v} \\ \|\mathbf{v}\| \end{bmatrix}. \quad (13)$$

Here, we assume $\|\mathbf{v}\| > 0$ and hence, the above system is well-defined.

It is obvious that the first row in Eq. (13) is the same as the original Eq. (12), but the inclusion of the second row in Eq. (13) gives us a Minkowskian structure of the augmented state variables of $\mathbf{X} := (\mathbf{v}^T, \|\mathbf{v}\|)^T$, which satisfies the cone condition:

$$\mathbf{X}^T \mathbf{g} \mathbf{X} = 0, \tag{14}$$

where

$$\mathbf{g} = \begin{bmatrix} \mathbf{I}_n & \mathbf{0}_{n \times 1} \\ \mathbf{0}_{1 \times n} & -1 \end{bmatrix} \tag{15}$$

is a Minkowski metric. \mathbf{I}_n is the identity matrix of order n , and the superscript T denotes the transpose. In terms of $(\mathbf{x}^T, \|\mathbf{x}\|)$, Eq. (14) holds, as

$$\mathbf{X}^T \mathbf{g} \mathbf{X} = \mathbf{v} \cdot \mathbf{v} - \|\mathbf{v}\|^2 = \|\mathbf{v}\|^2 - \|\mathbf{v}\|^2 = 0, \tag{16}$$

where the dot between two n -dimensional vectors represents their Euclidean inner product. The cone condition is thus the most natural constraint that we can impose on the dynamical system (13).

Consequently, we have an $n+1$ -dimensional augmented system:

$$\dot{\mathbf{X}} = \mathbf{A} \mathbf{X} \tag{17}$$

with a constraint (14), where

$$\mathbf{A} := \begin{bmatrix} \mathbf{0}_{n \times n} & \frac{\mathbf{f}(\mathbf{v}, \tau)}{\|\mathbf{v}\|} \\ \frac{\dot{\mathbf{f}}^T(\mathbf{v}, \tau)}{\|\mathbf{v}\|} & 0 \end{bmatrix} \tag{18}$$

is an element of the Lie algebra $so(n,1)$ of the proper orthochronous Lorentz group $SO_o(n,1)$, satisfying

$$\mathbf{A}^T \mathbf{g} + \mathbf{g} \mathbf{A} = 0. \tag{19}$$

This fact prompts us to employ the group preserving scheme, and its discretized mapping \mathbf{G} exactly preserves the following properties:

$$\mathbf{G}^T \mathbf{g} \mathbf{G} = \mathbf{g}, \tag{20}$$

$$\det \mathbf{G} = 1, \tag{21}$$

$$G_0^0 > 0, \tag{22}$$

where G_0^0 is the 00th component of \mathbf{G} . Such \mathbf{G} is an element of $SO_o(n,1)$.

Although the dimension of the new system rises by one, it has been shown that the new system has the advantage of admitting a GPS given as follows [Liu (2001)]:

$$\mathbf{X}_{\ell+1} = \mathbf{G}(\ell)\mathbf{X}_\ell, \tag{23}$$

where \mathbf{X}_ℓ stands for the numerical evaluation of \mathbf{X} at the discrete time τ_ℓ , and $\mathbf{G}(\ell) \in SO_o(n,1)$ is the group evaluation at time τ_ℓ .

In order to give a step by step numerical scheme, we suppose that $\mathbf{A}(\ell)$ in Eq. (19) is a constant matrix, taking its value at the ℓ -th step. An exponential mapping of $\mathbf{A}(\ell)$ for the interval $\tau_\ell \leq \tau < \tau_\ell + \Delta\tau$, when the time parameter τ in Eq. (18) is approximately fixed as $\tau = \tau_\ell$, admits:

$$\mathbf{G}(\ell) = \exp[\Delta\tau\mathbf{A}(\ell)] = \begin{bmatrix} \mathbf{I}_n + \frac{(a_\ell-1)}{\|\mathbf{f}_\ell\|^2} \mathbf{f}_\ell \mathbf{f}_\ell^T & \frac{b_\ell \mathbf{f}_\ell}{\|\mathbf{f}_\ell\|} \\ \frac{b_\ell \mathbf{f}_\ell^T}{\|\mathbf{f}_\ell\|} & a_\ell \end{bmatrix}, \tag{24}$$

where

$$a_\ell := \cosh\left(\frac{\Delta\tau \|\mathbf{f}_\ell\|}{\|\mathbf{v}_\ell\|}\right), \quad b_\ell := \sinh\left(\frac{\Delta\tau \|\mathbf{f}_\ell\|}{\|\mathbf{v}_\ell\|}\right). \tag{25}$$

For saving notation, we use $\mathbf{f}_\ell = f(\mathbf{v}_\ell, \tau_\ell)$. Substituting Eq. (24) for $\mathbf{G}(\ell)$ into Eq. (23) and taking its first row, we obtain

$$\mathbf{v}_{\ell+1} = \mathbf{v}_\ell + \frac{(a_\ell - 1)\mathbf{f}_\ell \cdot \mathbf{v}_\ell + b_\ell \|\mathbf{v}_\ell\| \|\mathbf{f}_\ell\|}{\|\mathbf{f}_\ell\|^2} \mathbf{f}_\ell = \mathbf{v}_\ell + \eta_\ell \mathbf{f}_\ell, \tag{26}$$

where η_ℓ is an adaptive factor. From $\mathbf{f}_\ell \cdot \mathbf{v}_\ell \geq -\|\mathbf{f}_\ell\| \|\mathbf{v}_\ell\|$, we can prove that

$$\eta_\ell \geq \left[1 - \exp\left(-\frac{\Delta\tau \|\mathbf{f}_\ell\|}{\|\mathbf{v}_\ell\|}\right)\right] \frac{\|\mathbf{v}_\ell\|}{\|\mathbf{f}_\ell\|} > 0, \quad \forall \Delta\tau > 0. \tag{27}$$

This scheme is group properties preserved for all $\Delta\tau > 0$, and is called the group preserving scheme.

3.3 The convergent criterion

We use the above GPS to integrate Eq. (11) from $\tau = 0$ to a selected fictitious final time τ_f . In the numerical integration process, we can examine the convergence of $v_{i,j,k,\ell}$ at the q - and $q + 1$ -steps by

$$\sqrt{\sum_{\ell=1}^{m_1} \sum_{i,j,k=1}^m [v_{i,j,k,\ell}^{q+1} - v_{i,j,k,\ell}^q]^2} \leq \varepsilon, \tag{28}$$

where ε is a selected criterion, m_1 is the number of subintervals in time direction, and m is the number of grid points in each spatial direction, presuming the same. If at a time $\tau_0 \leq \tau_f$ the above criterion is satisfied, then the solution of u is given by

$$u_{i,j,k,\ell} = \frac{v_{i,j,k,\ell}(\tau_0)}{1 + \tau_0}. \tag{29}$$

In practical, if a suitable τ_f is selected, we discover that the numerical solution is also approached very well to the true solution, even the above convergence criterion is not satisfied. The coefficient ψ introduced in Eq. (11) can enhance the stability of numerical integration.

Particularly, we would stress that the present approach is a new FTIM, which can calculate the parabolic PDE very effectively and stably. In the next section, we give six numerical examples to display some advantages of the proposed FTIM.

4 Numerical examples

We will apply the FTIM to the calculations of BHCP through numerical examples. We are interested in the stability of our approach when the input final measured data are polluted by random noise for different problems. We can evaluate the stability by increasing the different levels of random noise in the final data:

$$\hat{\mathbf{v}}_F = \mathbf{v}_F + sR(i), \tag{30}$$

where \mathbf{v}_F are the final exact data. We use the function RANDOM_NUMBER given in Fortran to generate the noisy data $R(i)$, which are random numbers in $[-1, 1]$, and s means the level of absolute noise. Then, the final noisy data $\hat{\mathbf{v}}_F$ are employed in the calculations.

4.1 Example 1

The following one-dimensional nonhomogeneous BHCP is considered:

$$u_t = u_{xx} + 2e^t \sin(x), \quad 0 < x < \pi, \quad 0 < t < T, \tag{31}$$

with the boundary conditions

$$u(0,t) = u(\pi,t) = 0, \tag{32}$$

and the final time condition

$$u(x,T) = e^T \sin(x). \tag{33}$$

The data to be retrieved are given by

$$u(x,t) = e^t \sin(x), \quad 0 \leq t < T. \tag{34}$$

A straightforward derivation according to the concept of FTIM results in

$$\dot{\mathbf{v}}_{i,\ell} = \frac{-\Psi}{\Delta t} [\mathbf{v}_{i,\ell+1} - \mathbf{v}_{i,\ell}] + \frac{\Psi}{(\Delta x)^2} [\mathbf{v}_{i+1,\ell} - 2\mathbf{v}_{i,\ell} + \mathbf{v}_{i-1,\ell}] + \Psi(1 + \tau)g_{i,\ell} + \frac{\mathbf{v}_{i,\ell}}{1 + \tau}, \tag{35}$$

where

$$\mathbf{v}_{0,\ell}(\tau) = \mathbf{v}_{1,\ell}(\tau) = 0, \tag{36}$$

$$\mathbf{v}_{i,m}(\tau) = (1 + \tau)e^T \sin(x_i). \tag{37}$$

Let us investigate some very severely ill-posed cases of this benchmark BHCP, where $T = 10$ are employed such that when the final data are in the order of $O(10^4)$, we attempt to use the FTIM to retrieve the desired initial data of $\sin x$, which are in the order of $O(1)$. Under the following parameters: $m = 20, m_1 = 20, \varepsilon = 10^{-6}, \Psi = 10^{-4}$, and a fictitious terminal time $\tau_f = 0.2$, and starting from an initial value of $\mathbf{v}_{i,\ell} = 4.95 \times 10^{-6} \sin(x_i)e^{10}$ because we know the final data in Eq. (33), we tackle this problem by our approach of FTIM with a fictitious time stepsize $\Delta\tau = 0.002$. Fig. 1 demonstrates the numerical results and numerical errors, and the maximum error is about 10^{-5} . Upon comparing with the numerical results in [Trong and Tuan (2006); Trong and Tuan (2008a)] with that from the quasi-reversibility method (see Table 1 of the above cited papers) and Chang and Liu (2010b) with the BGPS, we can say that the FTIM does not need to use the regularization technique and still acquire good results.

In Fig. 2, we show the numerical results and numerical errors for a final time $T = 10$ and with a noise of $s = 1$. The maximum error as displayed is in the order of 10^{-5} even for a larger disturbance with $s = 1$. The present results are also better than that calculated by Chang and Liu (2010b), of which the maximum error is 0.1, under a noise of $s = 0.002$. To the authors' best knowledge, there has been no open report that the numerical methods can calculate this severely ill-posed BHCP very well as the FTIM.

4.2 Example 2

Let us consider another one-dimensional nonhomogeneous BHCP:

$$u_t = u_{xx} - 2e^{-(x+t)}, \quad 0 < x < \pi, \quad 0 < t < T, \tag{38}$$

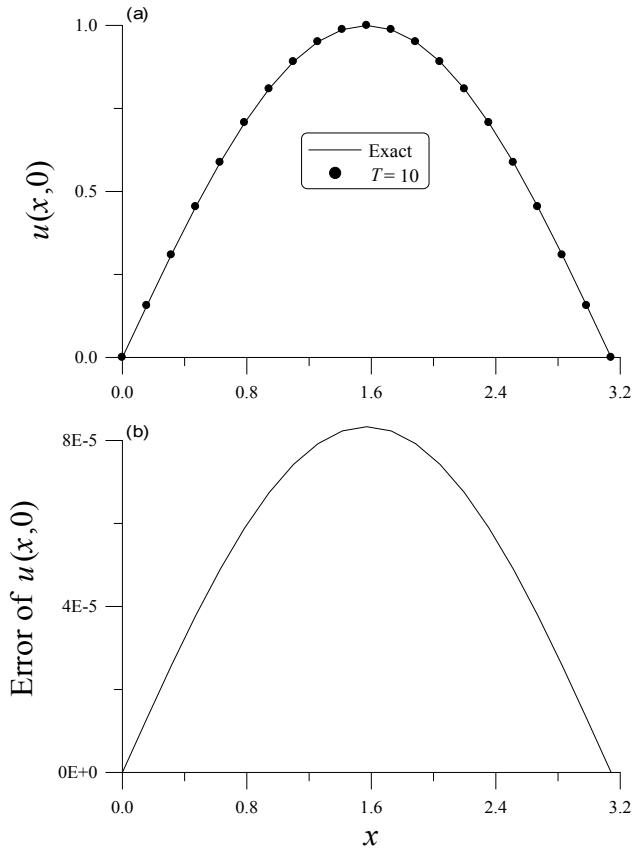


Figure 1: Comparisons of the exact solutions and numerical solutions for Example 1 with $T = 10$, and the corresponding numerical errors.

with the time varying boundary conditions

$$u(0,t) = e^{-t}, u(\pi,t) = e^{-(\pi+t)}, \quad (39)$$

and the final time condition

$$u(x,T) = e^{-(x+T)}. \quad (40)$$

The exact solution is given by

$$u(x,t) = e^{-(x+t)}. \quad (41)$$

Under the following parameters: $m = 80$, $m_1 = 20$, $\varepsilon = 10^{-6}$, $\psi = 10^{-4}$, and a fictitious terminal time $\tau_f = 0.001$, and starting from an initial value of $\mathbf{v}_{i,\ell} = 3.27 \times$

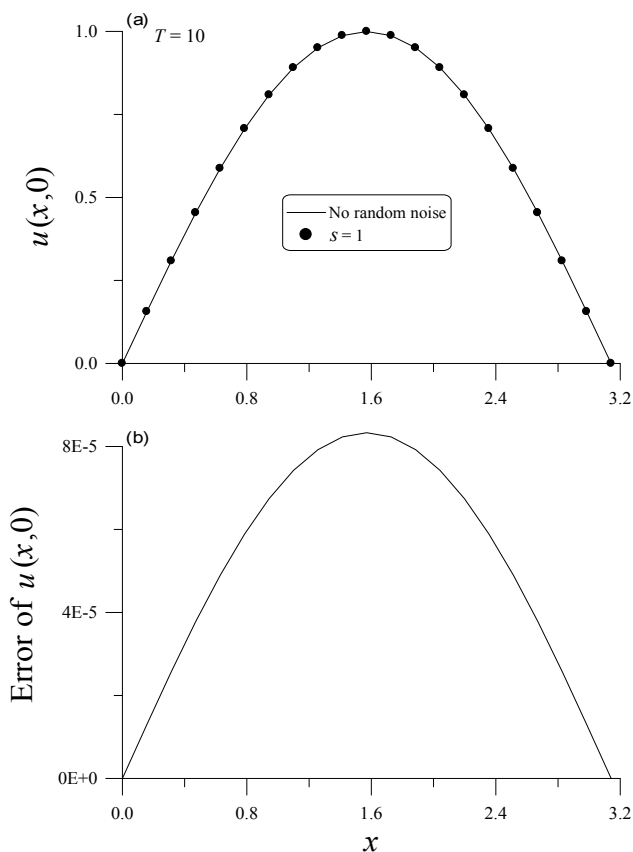


Figure 2: Comparisons of numerical solutions for Example 1 with different levels of noise $s = 0, 1$, and the corresponding numerical errors.

$10^6 e^{-(x_i+15)}$, we integrate Eq. (35) by using the GPS with a fictitious time stepsize $\Delta\tau = 0.001$.

Fig. 3 shows the numerical results and numerical errors for the final time of $T = 15$, and the maximum error is about 2.78×10^{-4} . Upon comparing with the numerical results of $T = 0.1$ in [Feng, Qian and Fu (2008)] with that from the Tikhonov regularization method (see Figs. 4 and 5 of the above cited paper), and the BGPS with $T = 10$ in [Chang and Liu (2010b)], we can say that the FTIM does not require to utilize the regularization technique and still acquire good results.

In this example, adding a large noisy disturbance with $s = 1$ on the input final data, we depicted the numerical result in Fig. 4(a) by the dotted line. Note that the accuracy is better than [Feng, Qian and Fu (2008)] even under a disturbance.

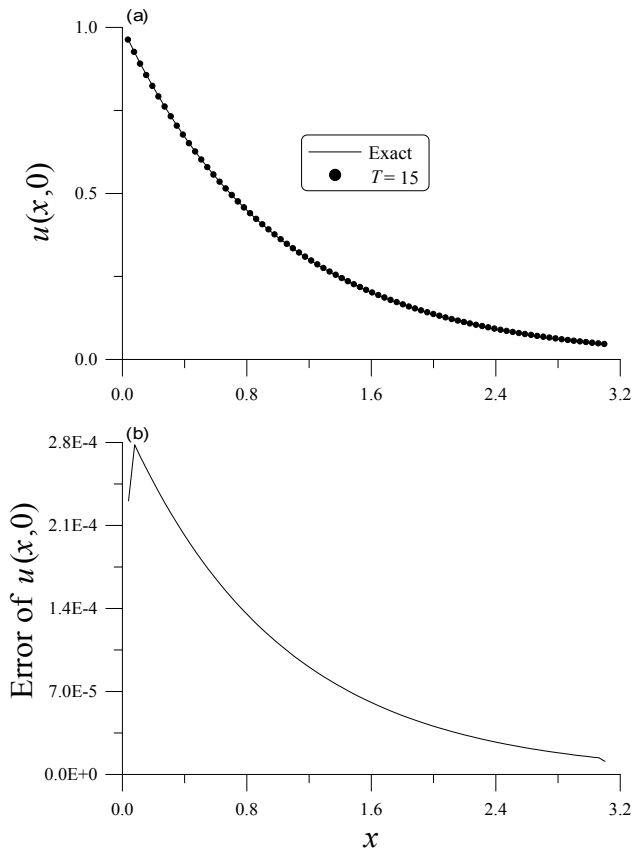


Figure 3: Comparisons of the exact solutions and numerical solutions for Example 2 with $T = 15$, and the corresponding numerical errors.

Moreover, the current results are also better than that calculated by Chang and Liu (2010b), of which the final time is 0.1 and the maximum error is 0.046, under a noise of $s = 0.006$.

4.3 Example 3

The following one-dimensional nonlinear BHCP is considered:

$$u_t = u_{xx} + F(u) + 2e^t \sin(x) - e^{4t} \sin^4(x), \quad 0 < x < \pi, \quad 0 < t < T, \tag{42}$$

with the boundary conditions

$$u(0,t) = u(\pi,t) = 0, \tag{43}$$

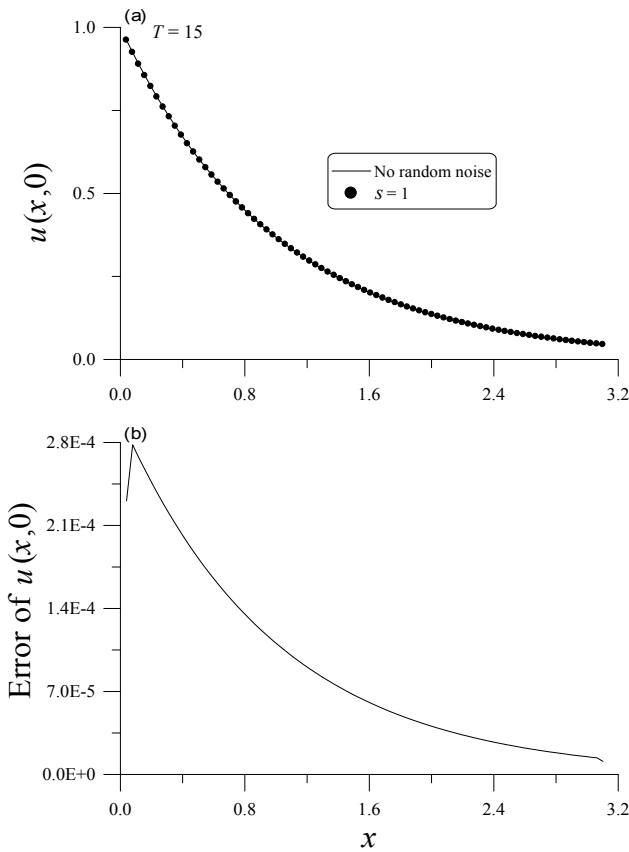


Figure 4: Comparisons of numerical solutions for Example 2 with different levels of noise $s = 0, 1$, and the corresponding numerical errors.

and the final time condition

$$u(x, T) = e^T \sin(x), \tag{44}$$

where $F(u) = u^4$, $u \in [-e^{10}, e^{10}]$.

The data to be recovered are given by

$$u(x, t) = e^t \sin(x), \quad 0 \leq t < T. \tag{45}$$

Under the following parameters: $m = 20$, $m_1 = 20$, $\varepsilon = 10^{-7}$, $\psi = 10^{-7}$, and a fictitious terminal time $\tau_f = 10^{-13}$, and starting from an initial value of $\mathbf{v}_{i,\ell} = 5.5 \times 10^{-4} \sin(x_i) e^{7.5}$, we solve this problem by the FTIM with a fictitious time stepsize

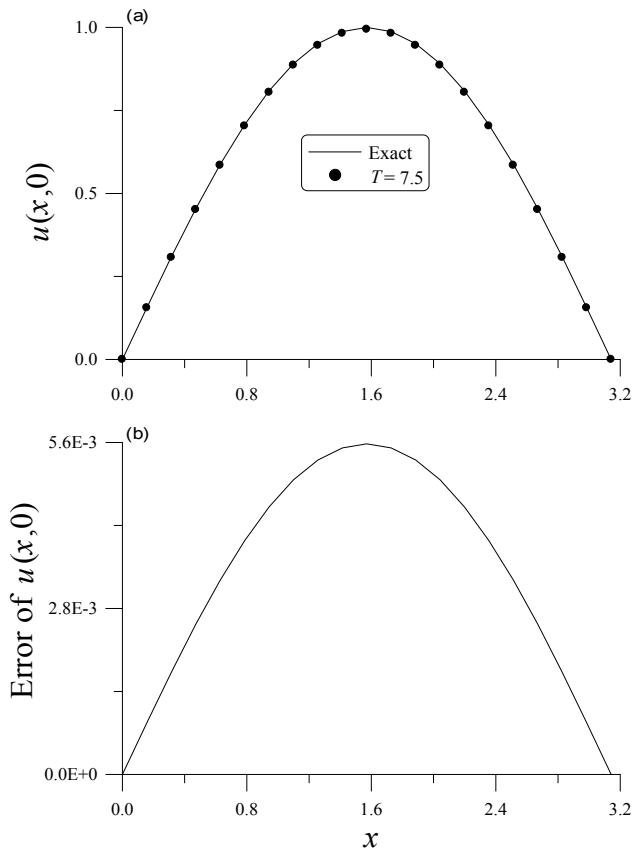


Figure 5: Comparisons of the exact solutions and numerical solutions with the final time $T = 7.5$, and the corresponding numerical errors.

$\Delta\tau = 10^{-14}$. Fig. 5 displays the numerical results and numerical errors for the final time of $T = 7.5$ with the order of $O(10^3)$. Upon comparing with the numerical results in [Trong and Tuan (2009a)] with that from the method of integral equation (see Table 2 of the above cited paper), in [Nam (2010)] with that from the truncation method (see Table 1 of the above cited paper), and in [Chang and Liu (2010b)] with that from the BGPS (see Figure 11 of the above cited paper), we can say that the FTIM does not require to utilize those complicated procedures (e.g., the regularization technique, the method of integral equation) and still acquire good results. In Fig. 5(b), the accuracy is the order of 10^{-3} .

We plotted the numerical result of $T = 7.5$ with adding an absolute noise with level $s = 1$ on the input final data in Fig. 6(a) by the dotted line. Note that the accuracy is

still in the order of 10^{-3} even under a large disturbance. Furthermore, the present results are also better than that calculated by Chang and Liu (2010b), of which the final time is 0.25 and the maximum error is 0.015, under a noise of $s = 0.001$.

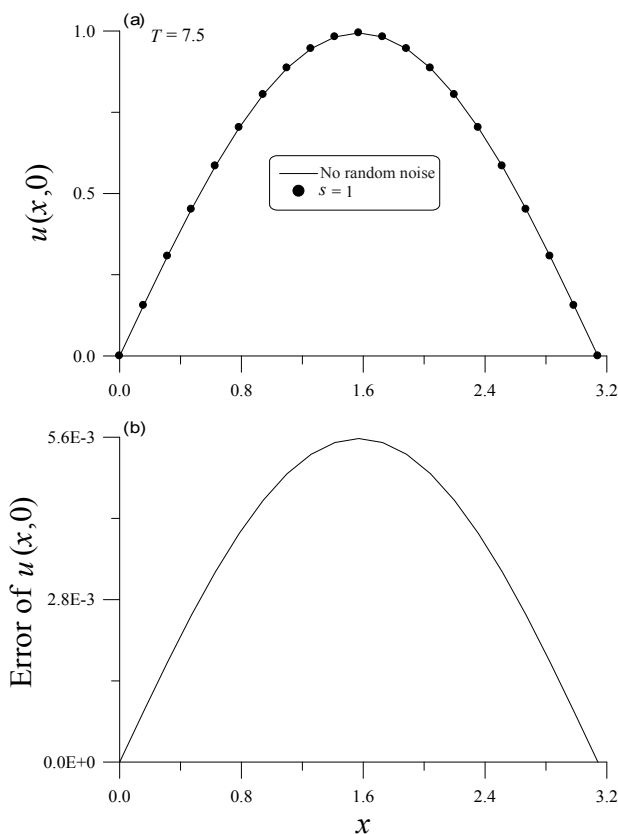


Figure 6: Comparisons of numerical solutions were made in (a) with different levels of noise $s = 0, 1$, and (b) the corresponding numerical errors.

4.4 Example 4

Let us consider the two-dimensional nonhomogeneous BHCP:

$$u_t = u_{xx} + u_{yy} + 3e^t \sin(x)\sin(y), \quad 0 < x < \pi, \quad 0 < y < \pi, \quad 0 < t < T, \quad (46)$$

with the boundary conditions

$$u(0, y, t) = u(\pi, y, t) = u(x, 0, t) = u(x, \pi, t) = 0, \quad (47)$$

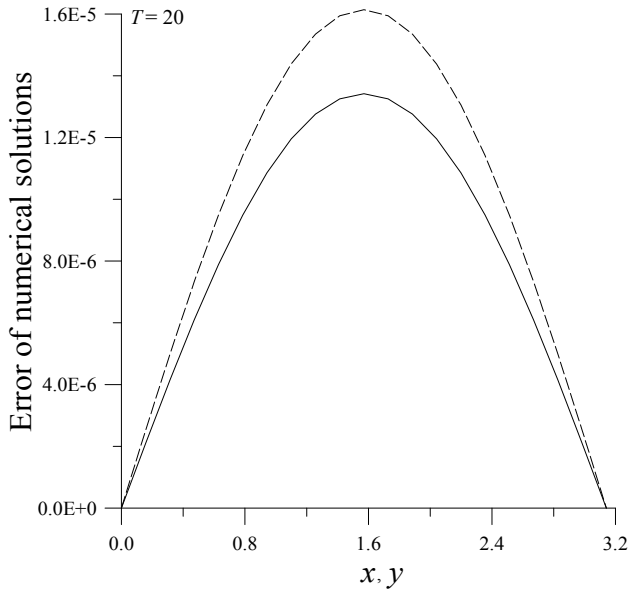


Figure 7: The errors of FTIM solutions for Example 4 with $T = 20$.

and the final time condition

$$u(x, y, T) = e^T \sin(x) \sin(y). \quad (48)$$

The exact solution is given by

$$u(x, y, t) = e^t \sin(x) \sin(y). \quad (49)$$

A derivation according to the FTIM leads to

$$\begin{aligned} \dot{\mathbf{v}}_{i,j,\ell} = & \frac{-\psi}{\Delta t} [v_{i,j,\ell+1} - v_{i,j,\ell}] + \frac{\psi}{(\Delta x)^2} [v_{i+1,j,\ell} - 2v_{i,j,\ell} + v_{i-1,j,\ell}] \\ & + \frac{\psi}{(\Delta y)^2} [v_{i,j+1,\ell} - 2v_{i,j,\ell} + v_{i,j-1,\ell}] + \psi(1 + \tau)g_{i,j,\ell} + \frac{v_{i,j,\ell}}{1 + \tau}. \end{aligned} \quad (50)$$

Under the following parameters: $m = 20$, $m_1 = 20$, $\varepsilon = 10^{-5}$, $\psi = 10^{-3}$, $T = 20$, and a fictitious terminal time $\tau_f = 3.04 \times 10^{-11}$, and starting from an initial value of $v_{i,j,\ell} = 1.97 \times 10^{-9} \cdot e^{20} \sin(x_i) \sin(y_j)$, we integrate Eq. (50) by using the GPS with a fictitious time stepsize $\Delta \tau = 10^{-14}$.

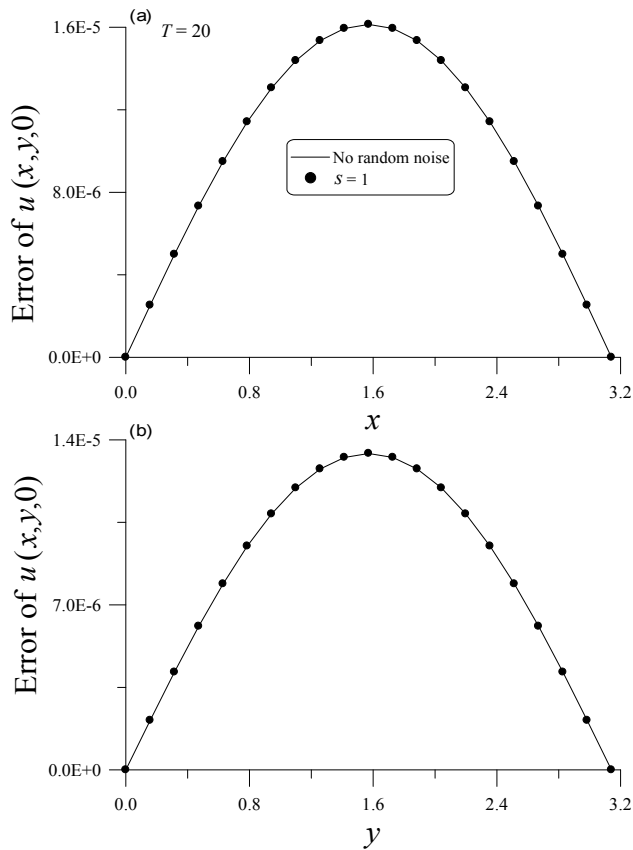


Figure 8: The numerical errors of FTIM solutions with and without random noise effect for Example 4 are plotted in (a) with respect to x at fixed $y = \pi/3$, and in (b) with respect to y at fixed $x = \pi/4$.

Fig. 7 indicates the errors of numerical solutions obtained from the FTIM for the case of $T = 20$, and the final data are very large in the order of $O(10^9)$. However, we can use the FTIM to retrieve the desired initial data $\sin x \sin y$, which are in the order of $O(1)$. At the point $x = 4\pi/20$, the error is plotted with respect to y by a dashed line, and at the point $y = 5\pi/20$, the error is plotted with respect to x by a solid line. The latter one is smaller than the former one because the point $y = 5\pi/20$ is near the boundary. However, the errors are smaller than that calculated by Tuan and Trong (2009) as shown in Table 1 and Chang and Liu (2010b) as shown in Figure 13 therein. For this very difficult problem, the FTIM proposed here is still good with a maximum error 1.6×10^{-5} .

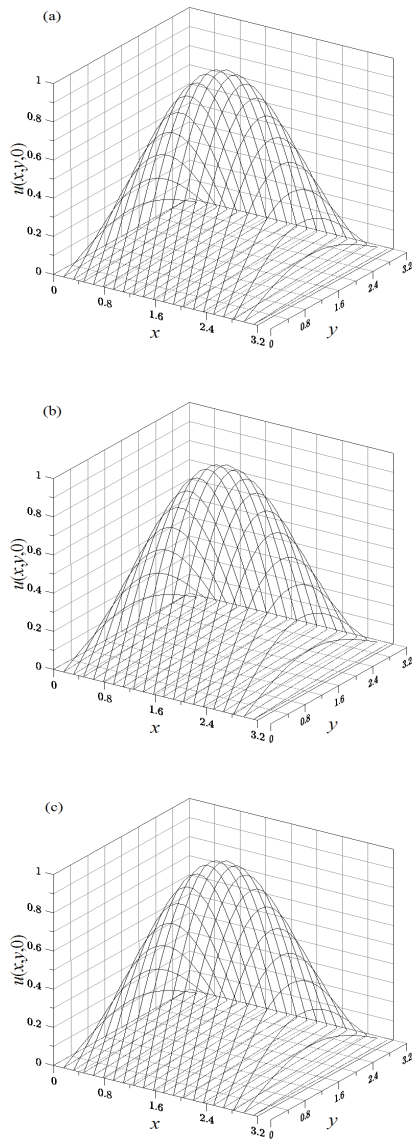


Figure 9: The exact solution for Example 4 of two-dimensional nonhomogeneous BHCP with $T = 20$ are shown in (a), in (b) the FTIM solution without random noise effect, and in (c) the FTIM solution with random noise.

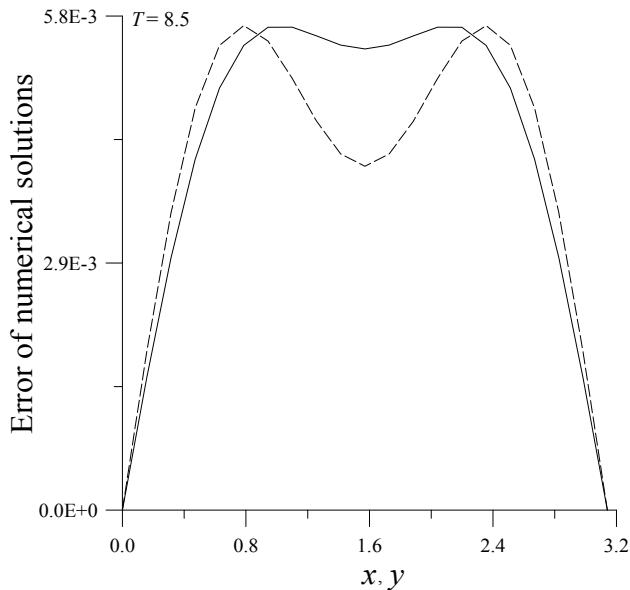


Figure 10: The errors of FTIM solutions for Example 5 with $T = 8.5$.

Recently, the numerical results have been calculated by Chang and Liu (2010b), of which the final time was 0.25 and the maximum error was 9.6×10^{-3} , under a noise of $s = 0.0002$. In Fig. 8, we compare the numerical errors with $T = 20$ for two cases: one without the random noise and the other with the absolute random noise in the level of $s = 1$. The exact solutions and numerical solutions are plotted in Figs. 9(a)-(c) sequentially. Even under the large noise, the numerical solution displayed in Fig. 9(c) is a good approximation to the exact initial data as shown in Fig. 9(a).

4.5 Example 5

Let us then consider the simple two-dimensional Allen-Cahn equation:

$$u_t = u_{xx} + u_{yy} + u - u^3 + 2e^t \sin(x)\sin(y) + e^{3t} \sin^3(x)\sin^3(y),$$

$$0 < x < \pi, 0 < y < \pi, 0 < t < T, \quad (51)$$

with the boundary conditions

$$u(0, y, t) = u(\pi, y, t) = u(x, 0, t) = u(x, \pi, t) = 0, \quad (52)$$

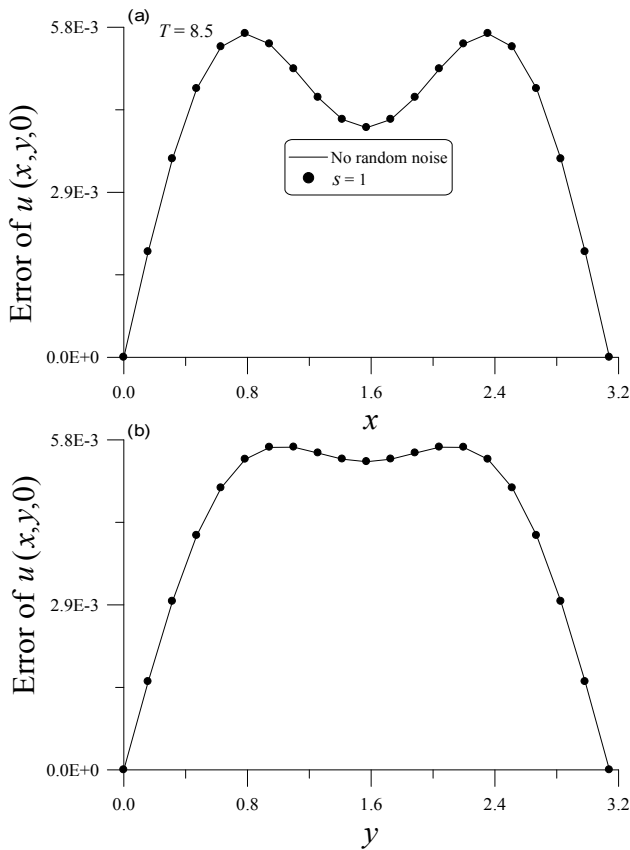


Figure 11: The numerical errors of FTIM solutions with and without random noise effect for Example 5 are plotted in (a) with respect to x at fixed $y = \pi/3$, and in (b) with respect to y at fixed $x = \pi/4$.

and the final time condition

$$u(x,y,T) = e^T \sin(x)\sin(y). \tag{53}$$

The exact solution is given by

$$u(x,y,t) = e^t \sin(x)\sin(y). \tag{54}$$

Under the following parameters: $m = 20$, $m_1 = 20$, $\varepsilon = 10^{-3}$, $\psi = 10^{-4}$, $T = 8.5$, and a fictitious terminal time $\tau_f = 1.91 \times 10^{-13}$, and starting from an initial value of $v_{i,j,\ell} = 2.0 \times 10^{-4} \cdot e^{8.5} \sin(x_i) \sin(y_j)$, we tackle this problem by our approach with a fictitious time stepsize $\Delta\tau = 10^{-15}$.

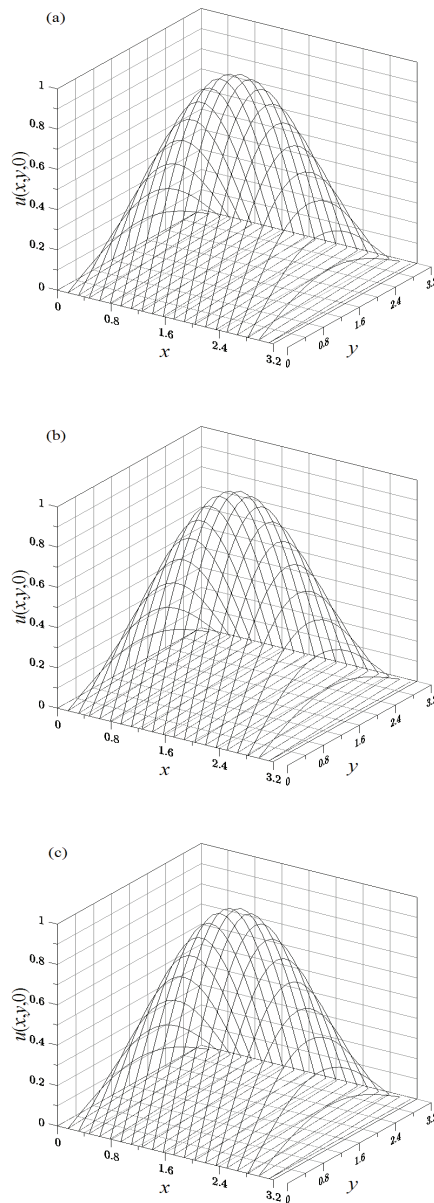


Figure 12: The exact solution for Example 5 of two-dimensional nonlinear BHCP with $T = 8.5$ are shown in (a), in (b) the FTIM solution without random noise effect, and in (c) the FTIM solution with random noise.

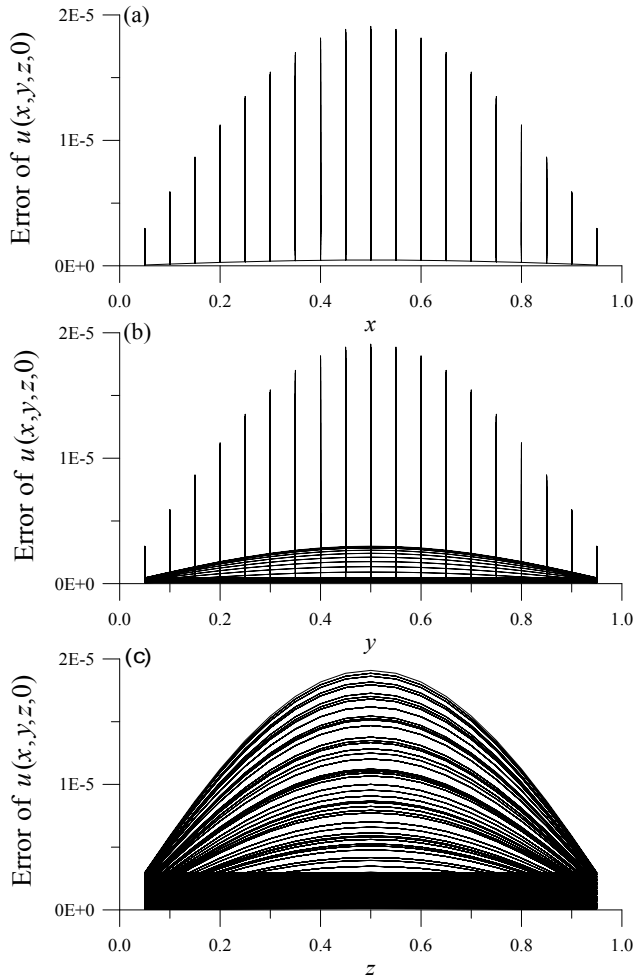


Figure 13: The numerical errors of FTIM solutions for Example 6 with $T = 5$ and $s = 1$ are plotted in (a) with respect to x by the errors projected along the yz -axes, (b) with respect to y by the errors projected along the xz -axes, and in (c) with respect to z by the errors projected along the xy -axes.

Fig. 10 presents the errors of numerical solutions obtained from the FTIM for the case of $T = 8.5$, and the final data are large in the order of $O(10^4)$. However, we can use the FTIM to retrieve the desired initial data $\sin x \sin y$, which are in the order of $O(1)$. At the point $x = 4\pi/20$, the error is plotted with respect to y by a dashed line, and at the point $y = 5\pi/20$, the error is plotted with respect to x by a solid line. The

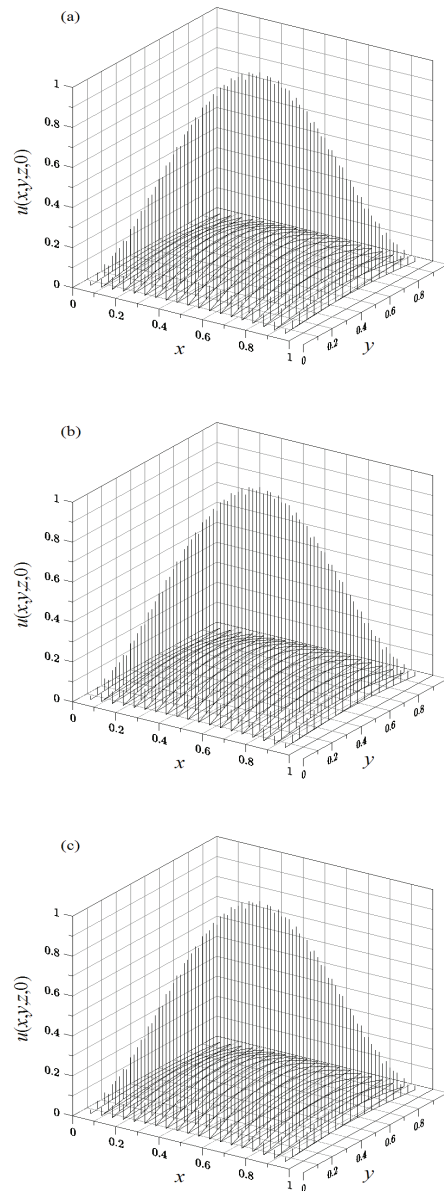


Figure 14: The exact solution for Example 6 of three-dimensional nonhomogeneous BHCP with $T = 5$ are shown in (a), in (b) the FTIM solution without random noise effect, and in (c) the FTIM solution with random noise.

latter one is smaller than the former one because the point $y = 5\pi/20$ is near the boundary. Nevertheless, the errors are smaller than that calculated by Trong and Tuan (2009b) as shown in Table 1 and Chang and Liu (2010b) as shown in Figure 16 therein. For this difficult problem, the FTIM proposed here is still good with a maximum error 5.67×10^{-3} .

The numerical results were calculated by Chang and Liu (2010b), of which the final time was 0.25 and the maximum error was 9.6×10^{-3} , under a noise of $s = 0.0002$. In Fig. 11, we compare the numerical errors with $T = 8.5$ for two cases: one without the random noise and the other with the absolute random noise in the level of $s = 1$. The exact solutions and numerical solutions are drawn in Figs. 12(a)-(c) sequentially. Even under the large noise, the numerical solution displayed in Fig. 12(c) is a good approximation to the exact initial data as shown in Fig. 12(a).

4.6 Example 6

Let us consider a three-dimensional BHCP:

$$u_t = u_{xx} + u_{yy} + u_{zz} + 4\pi^2 e^{\pi^2 t} \sin(\pi x) \sin(\pi y) \sin(\pi z),$$

$$0 < x < 1, 0 < y < 1, 0 < z < 1, 0 < t < T, \quad (55)$$

with the boundary conditions

$$u(0, y, z, t) = u(1, y, z, t) = u(x, 0, z, t) = u(x, 1, z, t) = u(x, y, 0, t) = u(x, y, 1, t) = 0,$$

$$(56)$$

and the final time condition

$$u(x, y, z, T) = e^{\pi^2 T} \sin(\pi x) \sin(\pi y) \sin(\pi z). \quad (57)$$

The exact solution is given by

$$u(x, y, z, t) = e^{\pi^2 t} \sin(\pi x) \sin(\pi y) \sin(\pi z). \quad (58)$$

Under the following parameters: $m = 20, m_1 = 20, \varepsilon = 10^{-4}, \psi = 10^{-4}, T = 5$, and a fictitious terminal time $\tau_f = 3 \times 10^{-26}$, and starting from an initial value of $v_{i,j,k,\ell} = 3.69 \times 10^{-22} \cdot e^{5\pi^2} \sin(\pi x_i) \sin(\pi y_j) \sin(\pi z_k)$, we resolve this problem by our approach with a fictitious time stepsize $\Delta\tau = 10^{-29}$. However, we can use the FTIM to recover the desired initial data $\sin\pi x \sin\pi y \sin\pi z$, which are in the order of $O(1)$. The numerical error is plotted with respect to x by the errors projected along the yz -axes in Fig. 13(a), the numerical error is plotted with respect to y

by the errors projected along the xz -axes in Fig. 13(b), and the numerical error is plotted with respect to z by the errors projected along the xy -axes in Fig. 13(c). Furthermore, the errors are much smaller than those calculated by Chang and Liu (2010b) as shown in Figure 21 therein.

The exact solution and numerical solutions are plotted in Fig. 14(a)-(c) sequentially. Even under the noise the numerical solution displayed in Fig. 14(c) is a good approximation to the exact initial data as shown in Fig. 14(a). This example is a hard nonhomogeneous BHCP problem to examine the numerical performance of our novel numerical algorithms. However, to the authors' best knowledge, there has been no report that numerical methods can calculate this seriously ill-posed three-dimensional nonhomogeneous BHCP very well as our approach.

5 Conclusions

In this study, we have transformed the original parabolic equation into another parabolic type evolution equation by introducing a fictitious time variable, and adding a fictitious viscous damping coefficient to enhance the stability of numerical integration of the discretized equations by utilizing the GPS. In addition, we only needed spending a little of computational time for integrating the discretized equations to acquire solutions. By employing the FTIM, we can calculate the solution and retrieve the initial data very well with a high order accuracy. Six numerical examples of the BHCP are worked out, which display that our proposed algorithm is applicable to the very severely ill-posed BHCP. The numerical errors of our approach are in the order of $O(10^{-3})$ – $O(10^{-8})$. Moreover, those effects are very significant in the computations of three-dimensional BHCP. Therefore, it can be concluded that the present FTIM is very accurate, stable, effective, and insensitive to the disturbance on final data. Its numerical implementation is simple and the computation speed is fast.

Acknowledgement: The author would like to express his thanks to the National Science Council, ROC, for their financial supports under Grant Numbers, NSC 99-2218-E492-005.

References

- Ames, K. A.; Cobb, S. S. (1997): Continuous dependence on modeling for related Cauchy problems of a class of evolution equations. *J. Math. Anal. Appl.*, vol. 215, pp. 15–31.
- Chang, C.-W.; Liu, C.-S. (2009): A fictitious time integration method for backward advection-dispersion equation. *CMES: Computer Modeling in Engineering*

& Sciences, vol. 51, pp. 261–276.

Chang, C.-W.; Liu, C.-S. (2010a): A new algorithm for direct and backward problems of heat conduction equation. *Int. J. Heat Mass Transfer*, vol. 53, pp. 5552–5569.

Chang, C.-W.; Liu, C.-S. (2010b): A backward group preserving scheme for multi-dimensional backward heat conduction problems. *CMES: Computer Modeling in Engineering & Sciences*, vol. 59, pp. 239–274.

Chang, C.-W.; Liu, C.-S.; Chang, J.-R. (2009): A new shooting method for quasi-boundary regularization of multi-dimensional backward heat conduction problems. *J. Chinese Inst. Engineers*, vol. 32, pp. 307–318.

Chang, C.-W.; Liu, C.-S.; Chang, J.-R. (2010a): A quasi-boundary semi-analytical method for backward heat conduction problems. *J. Chinese Inst. Engineers*, vol. 33, pp. 163–175.

Chang, C.-W.; Liu, C.-S.; Chang, J.-R. (2010b): A quasi-boundary semi-analytical approach for two-dimensional backward heat conduction problems. *CMC: Computers, Materials & Continua*, vol. 15, pp. 45–66.

Chang, J.-R.; Liu, C.-S.; Chang, C.-W. (2007): A new shooting method for quasi-boundary regularization of backward heat conduction problems. *Int. J. Heat Mass Transfer*, vol. 50, pp. 2325–2332.

Chi, C.-C.; Yeih, W.; Liu, C.-S. (2009): A novel method for solving the Cauchy problem of Laplace equation using the fictitious time integration method. *CMES: Computer Modeling in Engineering & Sciences*, vol. 47, pp. 167–190.

Chiwiacowsky, L. D.; de Campos Velho, H. F. (2003): Different approaches for the solution of a backward heat conduction problem. *Inv. Prob. Eng.*, vol. 11, pp. 471–494.

Feng, X.-L.; Qian, Z.; Fu, C.-L. (2008): Numerical approximation of solution of nonhomogeneous backward heat conduction problem in bounded region. *Math. Comp. Simul.*, vol. 79, pp. 177–188.

Han, H.; Ingham, D. B.; Yuan, Y. (1995): The boundary element method for the solution of the backward heat conduction equation. *J. Comp. Phys.*, vol. 116, pp. 292–299.

Iijima, K. (2004): Numerical solution of backward heat conduction problems by a high order lattice-free finite difference method. *J. Chinese Inst. Engineers*, vol. 27, pp. 611–620.

Jourhmane, M.; Mera, N. S. (2002): An iterative algorithm for the backward heat conduction problem based on variable relaxation factors. *Inv. Prob. Eng.*, vol. 10, pp. 293–308.

Kirkup, S. M.; Wadsworth, M. (2002): Solution of inverse diffusion problems by operator-splitting methods. *Appl. Math. Model.*, vol. 26, pp. 1003–1018.

Ku, C.-Y.; Yeih, W.; Liu, C.-S.; Chi, C.C.; (2009): Applications of the fictitious time integration method using a new time-like function. *CMES: Computer Modeling in Engineering & Sciences*, vol. 43, pp. 173–190.

Lattés, R.; Lions, J. L. (1969): *The Method of Quasireversibility, Applications to Partial Differential Equations*. Elsevier, NY, USA.

Lesnic, D.; Elliott, L.; Ingham, D. B. (1998): An iterative boundary element method for solving the backward heat conduction problem using an elliptic approximation. *Inv. Prob. Eng.*, vol. 6, pp. 255–279.

Li, M.; Jiang, T.; Hon, Y. C. (2010): A meshless method based on RBFs method for nonhomogeneous backward heat conduction problem. *Eng. Anal. Bound. Elem.*, vol. 34, pp.785–792.

Liu, C.-S. (2001): Cone of non-linear dynamical system and group preserving schemes. *Int. J. of Non-Linear Mech.*, vol. 36, pp. 1047–1068.

Liu, C.-S. (2004): Group preserving scheme for backward heat conduction problems. *Int. J. Heat Mass Transfer*, vol. 47, pp. 2567–2576.

Liu, C.-S. (2006a): An efficient backward group preserving scheme for the backward in time Burgers equation. *CMES: Computer Modeling in Engineering & Sciences*, vol. 12, pp. 55–65.

Liu, C.-S. (2006b): One-step GPS for the estimation of temperature-dependent thermal conductivity. *Int. J. Heat Mass Transfer*, vol. 49, pp. 3084–3093.

Liu, C.-S. (2006c): An efficient simultaneous estimation of temperature-dependent thermophysical properties. *CMES: Computer Modeling in Engineering & Science*, vol. 14, pp. 77–90.

Liu, C.-S. (2008a): Solving an inverse Sturm-Liouville problem by a Lie-group method. *Bound. Value Prob.*, vol. 2008, Article ID 749865.

Liu, C.-S. (2008b): Identifying time-dependent damping and stiffness functions by a simple and yet accurate method. *J. Sound Vib.*, vol. 318, pp. 148–165.

Liu, C.-S. (2008c): A Lie-group shooting method for simultaneously estimating the time-dependent damping and stiffness coefficients. *CMES: Computer Modeling in Engineering & Science*, vol. 27, pp. 137–149.

Liu, C.-S. (2008d): A time-marching algorithm for solving non-linear obstacle problems with the aid of an NCP-function. *CMC: Computers, Materials & Continua*, vol. 8, pp. 53–65.

Liu, C.-S. (2008e): A fictitious time integration method for two-dimensional quasi-

linear elliptic boundary value problems. *CMES: Computer Modeling in Engineering & Science*, vol. 33, pp. 179–198.

Liu, C.-S.; Atluri, S. N. (2008a): A novel time integration method for solving a large system of non-linear algebraic equations. *CMES: Computer Modeling in Engineering & Science*, vol. 31, pp. 71–83.

Liu, C.-S.; Atluri, S. N. (2008b): A novel fictitious time integration method for solving the discretized inverse Sturm-Liouville problems, for specified eigenvalues. *CMES: Computer Modeling in Engineering & Science*, vol. 36, pp. 261–286.

Liu, C.-S.; Atluri, S. N. (2008c): A novel time integration method (FTIM) for solving mixed complementarity problems with applications to non-linear optimization. *CMES: Computer Modeling in Engineering & Science*, vol. 34, pp. 155–178.

Liu, C.-S.; Chang, J.-R.; Chang, K.-H.; Chen, Y.-W. (2008): Simultaneously estimating the time-dependent damping and stiffness coefficients with the aid of vibrational data. *CMC: Computers, Materials & Continua*, vol. 7, pp. 97–107.

Liu, C.-S. (2009): A fictitious time integration method for solving m -point boundary value problems. *CMES: Computer Modeling in Engineering & Science*, vol. 39, pp. 125–154.

Liu, C.-S.; Atluri, S. N. (2009): A fictitious time integration method for the numerical solution of the Fredholm integral equation and for numerical differentiation of noisy data, and its relation to the filter theory. *CMES: Computer Modeling in Engineering & Science*, vol. 41, pp. 243–261.

Liu, C.-S.; Chang, C.-W.; Chang, J.-R. (2006): Past cone dynamics and backward group preserving schemes for backward heat conduction problems. *CMES: Computer Modeling in Engineering & Sciences*, vol. 12, pp. 67–81.

Liu, J. (2002): Numerical solution of forward and backward problem for 2-D heat conduction equation. *J. Comp. Appl. Math.*, vol. 145, pp. 459–482.

Long, N. T.; Dinh, A. P. N. (1994): Approximation of parabolic non-linear evolution equation backward in time. *Inv. Prob.*, vol. 10, pp. 905–914.

Mera, N. S. (2005): The method of fundamental solutions for the backward heat conduction problem. *Inv. Prob. Sci. Eng.*, vol. 13, pp. 65–78.

Mera, N. S.; Elliott, L.; Ingham, D. B.; Lesnic, D. (2001): An iterative boundary element method for solving the one-dimensional backward heat conduction problem. *Int. J. Heat Mass Transfer*, vol. 44, pp. 1937–1946.

Mera, N. S.; Elliott, L.; Ingham, D. B. (2002): An inversion method with decreasing regularization for the backward heat conduction problem. *Num. Heat Transfer B*, vol. 42, pp. 215–230.

Muniz, W. B.; Ramos, F. M.; de Campos Velho, H. F. (2000): Entropy- and

Tikhonov-based regularization techniques applied to the backward heat equation. *Int. J. Comp. Math.*, vol. 40, pp. 1071–1084.

Muniz, W. B.; de Campos Velho, H. F.; Ramos, F. M. (1999): A comparison of some inverse methods for estimating the initial condition of the heat equation. *J. Comp. Appl. Math.*, vol. 103, pp. 145–163.

Nam, P. T. (2010): An approximate solution for nonlinear backward parabolic equations. *J. Math. Anal. Appl.*, vol. 367, pp. 337–349.

Showalter, R. E. (1983): Cauchy problem for hyper-parabolic partial differential equations. In *Trends in the Theory and Practice of Non-Linear Analysis*, Elsevier, Amsterdam, Netherlands, pp. 421–425.

Trong, D. D.; Quan, P. H.; Khanh, T. V.; Tuan, N. H. (2007): A nonlinear case of the 1-D backward heat problem: Regularization and error estimate. *Zeitschrift Anal. und ihre*, vol. 26, pp. 231–245.

Trong, D. D.; Tuan, N. H. (2006): Regularization and error estimates for nonhomogeneous backward heat problems. *Electron. J. Diff. Eq.*, vol. 2006, pp. 1–10.

Trong, D. D.; Tuan, N. H. (2008a): A nonhomogeneous backward heat problem: regularization and error estimates. *Electron. J. Diff. Eq.*, vol. 2008, pp. 1–14.

Trong, D. D.; Tuan, N. H. (2008b): Stabilized quasi-reversibility method for a class of nonlinear ill-posed problems. *Electron. J. Diff. Eq.*, vol. 2008, pp. 1–12.

Trong, D. D.; Tuan, N. H. (2009a): Regularization and error estimate for the nonlinear backward heat problem using a method of integral equation. *Nonlinear Anal.*, vol. 71, pp. 4167–4176.

Trong, D. D.; Tuan, N. H. (2009b): Remarks on a 2-D nonlinear backward heat problem using a truncated Fourier series method. *Electron. J. Diff. Eq.*, vol. 2009, pp. 1–13.

Tsai, C. H.; Young, D. L.; Kolibal J. (2010) : An analysis of backward heat conduction problems using the time evolution method of fundamental solutions. *CMES: Computer Modeling in Engineering & Sciences*, vol. 66, pp. 53–71.

Tuan, N. H.; Trong, D. D. (2009): A new regularized method for two dimensional nonhomogeneous backward heat problem. *Appl. Math. Comp.*, vol. 2008, pp. 1–14.